Percolation Transition in Supercritical Water: A Monte Carlo Simulation Study

ARTICLE *in* THE JOURNAL OF PHYSICAL CHEMISTRY B · AUGUST 2007

Impact Factor: 3.3 · DOI: 10.1021/jp070575j · Source: PubMed

4 AUTHORS, INCLUDING:

Pál Jedlovszky
Eszterházy Károly Fõiskola
171 PUBLICATIONS **2,912** CITATIONS
SEE PROFILE

Ivan V. Brovchenko
Technische Universität Dortmund
92 PUBLICATIONS **1,648** CITATIONS
SEE PROFILE

Alla Oleinikova
Technische Universität Dortmund
91 PUBLICATIONS **2,667** CITATIONS
SEE PROFILE

Percolation Transition in Supercritical Water: A Monte Carlo Simulation Study

Lívia B. Pártay and Pál Jedlovszky*

Laboratory of Interfaces and Nanosize Systems, Institute of Chemistry, Eötvös Loránd University, Pázmány Péter stny. 1/a, H-1117 Budapest, Hungary

Ivan Brovchenko and Alla Oleinikova

Department of Physical Chemistry, University of Dortmund, Otto Hahn str. 6, D-44227 Dortmund, Germany

Received: January 23, 2007; In Final Form: May 3, 2007

Computer simulations of water have been performed on the canonical ensemble at 15 different molecular number densities, ranging from 0.006 to 0.018 $Å^{-3}$, along the supercritical isotherm of 700 K, in order to characterize the percolation transition in the system. It is found that the percolation transition occurs at a somewhat higher density than what is corresponding to the supercritical extension of the boiling line. We have shown that the fractal dimension of the largest cluster and the probability of finding a spanning cluster are the most appropriate properties for the location of the true percolation threshold. Thus, percolation transition occurs when the fractal dimension of the largest cluster reaches 2.53, and the probability of finding a cluster that spans the system in at least one dimension and in all the three dimensions reaches 0.97 and 0.65, respectively. On the other hand, the percolation threshold cannot be accurately located through the cluster size distribution, as it is distorted by appearance of clusters crossing the finite simulated system even far below the percolation threshold. The structure of the largest water cluster is dominated by a linear, chainlike arrangement, which does not change noticeably until the largest cluster becomes infinite.

1. Introduction

The behavior of water in thermodynamic states above the critical point is in the focus of scientific interest for more than a decade.[1−54] The scientific importance of this subject lies in the fact that various properties of water (e.g., dielectric constant, viscosity, solvating ability, etc.) can be continuously varied in the supercritical region from values characteristic of a strongly associating system to gaslike values by controlling its density and connectivity by pressure and temperature, respectively. Thus, for instance, in certain supercritical states water can even act as a nonpolar solvent. This fact is also of technological importance,[52] since, for example, it enables supercritical water to be the medium of the environmentally friendly oxidation of hazardous organic wastes. The remarkably strong dependence of the properties of water on the thermodynamic conditions in supercritical states is ultimately originated in the breakdown of the three-dimensional space-filling percolation hydrogen-bonded network of the molecules, present at ambient conditions,[55,56] with increasing temperature and decreasing pressure. The geometry of the hydrogen bonds rapidly becomes distorted with increasing temperature in liquid water in various ways (e.g., the preference of the neighboring molecules for the tetrahedral arrangement around each other already disappears at relatively low temperatures;[26,34] the hydrogen bonds become gradually less linear with increasing temperature[22,26,35,57]), and thus the three-dimensional hydrogen-bonded network of the molecules becomes substantially destroyed.[58] However, in spite of these changes in the hydrogen-bonding structure, the water molecules are still forming an infinite percolating hydrogen-bonded network in liquid states at the vicinity of the critical point.[2,26,32,47]

In spite of some early claims of the contrary,[6,7,9] it is now widely accepted that a considerable number of hydrogen bonds still persist in water even above the critical point. This view is supported by neutron[22,23,26−28,48] and X-ray diffraction[2,14,15] experiments, nuclear magnetic resonance,[24] infrared,[1,3] Raman,[39] and microwave spectroscopy[33] measurements as well as by several computer simulation studies.[4,8,11−13,18−21,29−32,34−37] It has also been claimed that the infinite hydrogen-bonded network breaks down via percolation transition in supercritical water.[2,31,32,36,53,54] In a previous paper we suggested that the locus of the thermodynamic state points at which such a percolation transition occurs is the supercritical extension of the boiling line on the $p-T$ phase diagram.[53] However, in a recent study we have shown that there is a range of thermodynamic states in which the structure of water can be characterized by mesoscopic clusters that are large enough for spanning over the finite simulation box but by no means are infinite.[54] Since such mesoscopic clusters can easily be misidentified as infinite ones, the line of percolation of the hydrogen-bonded clusters has to be corrected toward higher pressures and densities. The line of the percolation transitions of the *physical* clusters should start at the critical point,[59] and it is expected to follow (or, at least, go close to) the extension of the boiling line in the supercritical region. The physical clusters, the definition of which also takes into account the relative kinetic energy of the molecules besides their relative potential energy,[60] are practically identical with the hydrogen-bonded clusters at ambient conditions; however, this is not the case above the critical temperature.

In this article, we present a detailed analysis of the percolation transition of the hydrogen-bonded water clusters along a supercritical isotherm. In the present set of simulations we have controlled the density rather than the pressure of the system, since the thermodynamic range that is characterized by the

* Corresponding author. E-mail: pali@chem.elte.hu.

10.1021/jp070575j CCC: $37.00
Published on Web 06/13/2007

TABLE 1: Properties of the Hydrogen-Bonded Water Clusters around the Percolation Threshold

			300 water system						1000 water system					
state	ρ/Å^{-3}	ρ/g cm^{-3}	d_f	$R^{(e)}$	$R^{(3)}$	$\langle S_w \rangle$*	n_{HB}	n_{HB}*	d_f	$R^{(e)}$	$R^{(3)}$	$\langle S_w \rangle$*	n_{HB}	n_{HB}*
A	0.0060	0.180		0.004	0.000	3.97	1.10	2.04		0.000	0.000	4.45	1.07	2.07
B	0.0070	0.210		0.010	0.000	4.40	1.18	2.05		0.000	0.000	5.54	1.18	2.09
C	0.0080	0.240		0.076	0.000	5.31	1.27	2.07		0.004	0.000	7.06	1.28	2.12
D	0.0090	0.269	1.80	0.304	0.010	6.54	1.42	2.12		0.036	0.000	8.85	1.37	2.13
E	0.0100	0.299	1.85	0.470	0.046	7.38	1.48	2.13		0.146	0.006	11.6	1.46	2.16
F	0.0105	0.314	1.86	0.530	0.072	7.80	1.50	2.13	1.6 9	0.326	0.018	13.3	1.51	2.17
G	0.0110	0.329	1.98	0.708	0.146	8.14	1.54	2.14	1.7 8	0.368	0.046	14.4	1.54	2.17
H	0.0115	0.344	2.06	0.824	0.218	8.69	1.60	2.15	1.9 0	0.590	0.090	16.4	1.59	2.18
I	0.0120	0.360	2.12	0.810	0.284	8.30	1.59	2.15	2.0 0	0.706	0.148	18.1	1.61	2.18
J	0.0125	0.374	2.34	0.954	0.504	7.87	1.68	2.18	2.1 7	0.876	0.364	19.3	1.66	2.20
K	0.0130	0.389	2.34	0.954	0.582	8.32	1.69	2.17	2.3 5	0.952	0.542	19.9	1.71	2.20
L	0.0135	0.404	2.42	0.952	0.636	8.63	1.72	2.18	2.4 1	0.974	0.646	19.7	1.73	2.20
M	0.0140	0.419	2.53	0.994	0.766	7.36	1.77	2.19	2.5 9	0.994	0.940	14.8	1.78	2.22
N	0.0150	0.449	2.66	1.000	0.896	5.81	1.83	2.21	2.7 2	1.000	0.966	9.00	1.85	2.24
O	0.0160	0.479	2.77	1.000	0.976	3.75	1.92	2.24	2.8 4	1.000	0.966	4.57	1.93	2.26

existence of mesoscopic water clusters might be rather narrow in terms of the pressure,[53] but it is certainly quite broad in terms of the density.[54] Further, direct application of the percolation theory suggests studying the clustering versus an occupancy variable, which is the density (and not the pressure) in the case of one-component fluids. Apart from the localization of the true three-dimensional percolation transition of supercritical water, a detailed analysis of the properties of mesoscopic water clusters is also given at densities below and above the percolation threshold. The effect of the finite size of the system simulated on the obtained results is discussed.

2. Computational Details

2.1. Monte Carlo Simulations. Monte Carlo simulations of supercritical water have been performed in the canonical (N, V, T) ensemble along the $T = 700$ K isotherm at 15 different molecular number density values ranging from 0.006 to 0.016 Å^{-3}. The densities corresponding to the different systems simulated (denoted by A−O) are summarized in Table 1. In order to investigate the effect of the finite size of the system on the percolation properties, the entire set of simulations has been performed both with 1000 and 300 molecules. Water molecules have been described by the SPC/E potential model,[61] since this model is known to reproduce the properties of water around the critical point considerably better than most of the other, conventionally used water potentials.[37,62] Cubic basic simulation box and standard periodic boundary conditions have been used. All interactions have been truncated to zero beyond the oxygen−oxygen distance of 15.0 Å and 10.0 Å in the case of the large and small systems, respectively. The long-range part of the electrostatic interactions has been accounted for using the reaction field correction method[63,64] under conducting boundary conditions. In a Monte Carlo step a randomly chosen water molecule has been randomly translated by no more than 0.2 Å and randomly rotated around a randomly chosen space-fixed axis by no more than 10°. The systems have been equilibrated by performing 10^4N Monte Carlo moves (N being the number of water molecules in the system). In the production stage 500 sample configurations per system, separated by $200N$ Monte Carlo steps each, have been saved for the analyses.

2.2. Definition of the Hydrogen Bonds and Clusters. Since we have previously found that the geometric and energetic definitions of the hydrogen-bonded water pairs lead to essentially the same behavior of the observed hydrogen-bonded clusters,[53] in the present study we only use a geometric definition of the hydrogen bond. Thus, two water molecules are regarded as hydrogen bonded if the distance between the closest oxygen−hydrogen pair is smaller than 2.5 Å, which corresponds to the position of the first minimum of the O−H partial pair correlation function at ambient conditions. This criterion assumes that the distance between the oxygen atoms of two water molecules is smaller than 3.5 Å, corresponding to the position of the first minimum of the O−O pair correlation function. Two molecules are regarded as belonging to the same cluster if they are connected by a chain of intact hydrogen bonds. Thus, a cluster is the assembly of all the water molecules that are connected to each other by hydrogen bonds. The size of the cluster S means the number of molecules belonging to it.

2.3. Detection of the Percolation Threshold. In order to detect the percolation threshold in the system, we have used four different methods.

2.3.1. Fractal Dimension. Since the largest cluster of the system is a fractal object above the percolation threshold, and no objects with the fractal dimension lower than 2.53 can be infinite in the three-dimensional space,[65] the true percolation threshold is located where the fractal dimension d_f of the largest cluster in the system reaches the critical value of 2.53. The fractal dimension of the largest cluster can be evaluated by fitting the cumulative radial distribution of its molecules as

$$m(r) \sim r^{d_f} \tag{1}$$

where $m(r)$ is the number of molecules that belong to the largest cluster and are located closer than the distance r from a given molecule of this cluster. We have recently demonstrated that the three-dimensional percolation threshold, i.e., where a truly infinite cluster appears in the system, can be detected in this way.[54]

2.3.2. Spanning Probability. Percolation transition can be detected through the critical probability of finding a cluster that spans the system. Since this critical spanning probability has a universal value that does not depend or very weakly depends on the size of the system once its dimensionality and boundary conditions as well as the spanning rule are set,[66] the percolation threshold is located at the point where the spanning probability values calculated in systems of different size become equal to each other. In this study we use two different spanning rules: the probability of finding a cluster that spans the system in at least one dimension $R^{(e)}$, and the probability of finding a cluster that spans the system in all the three dimensions $R^{(3)}$. Recently, we have shown that the critical value of $R^{(e)}$ is above 0.95 in the case of three-dimensional aqueous systems with standard periodic boundary conditions.[54,67]

2.3.3. Cluster Size Distribution. The distribution of the cluster size $P(S)$ obeys a power law at the percolation threshold:

$$P(S) \sim S^{-\tau} \tag{2}$$

with the universal exponent $\tau = 2.19$, in three-dimensional systems.[68] In systems that are below the percolation threshold the $P(S)$ distribution deviates down from eq 2 already at small cluster sizes. On the other hand, in percolating systems the $P(S)$ distribution strongly exceeds the critical line of eq 2 at large S values (this peak corresponds to the infinite water clusters), and drops below it before this peak, at intermediate cluster sizes. At the percolation threshold in finite system $P(S)$ follows eq 2 in a broad S range, up to where the linear extension of the cluster becomes comparable with the system size. Due to the fact that clusters with the linear extension exceeding the finite size of the system simulated cannot be observed, the population of the clusters with sizes close to the total number of the molecules in the system is overrepresented, and hence a hump of $P(S)$ appears at large S values even below the true percolation threshold.

2.3.4. Cluster Size Weight Average. The cluster size weight average $\langle S_w \rangle$, defined as[55,68]

$$\langle S_w \rangle = \frac{\sum_{S=1}^{N} S^2 P(S)}{\sum_{S=1}^{N} S P(S)} \tag{3}$$

(often denoted as $\langle n_w \rangle$, as well) passes through a maximum in finite systems just below the percolation threshold, if the largest cluster of the system is excluded from the sums of eq 3.[69] Contrary to the first three methods, the percolation threshold obviously cannot be accurately located through the cluster size weight average; only a lower limit of it can be given this way.

3. Results and Discussion

3.1. Localization of the Percolation Threshold. In order to calculate the fractal dimension of the largest cluster present in the system we have fitted eq 1 to the obtained $m(r)$ distribution of the molecules belonging to this cluster. The $m(r)$ functions resulted from the simulations and the fitted curves are shown in Figure 1, whereas the obtained d_f values are summarized in Table 1. As is seen from Figure 1, the obtained $m(r)$ function shows rapid increase in the entire r range within which it has been calculated (i.e., up to half of the edge length of the basic simulation box) only above the water number density values of 0.0080 and 0.0100 Å^{-3} (i.e., states C and E) in the systems containing 300 and 1000 water molecules, respectively. Up to these densities the $m(r)$ distribution of the largest cluster has an inflection point at a certain r value, and exhibits saturation above this point, indicating that this cluster is, on average, certainly smaller than the finite simulation box. Since the true fractal is an infinite object by definition, the evaluation of the fractal dimension of the largest cluster is of little meaning in these systems, and hence it has been omitted.

The variation of d_f with the density of the system is shown in Figure 2. As is seen from this figure and from Table 1, the obtained d_f values show a rather weak dependence on the size of the system, and the $d_f(\rho)$ curves obtained in the systems of different size intersect each other at the density of 0.0135 Å^{-3} (system L). This value is very close to the threshold density, which falls between 0.0135 and 0.0140 Å^{-3}, where d_f achieves

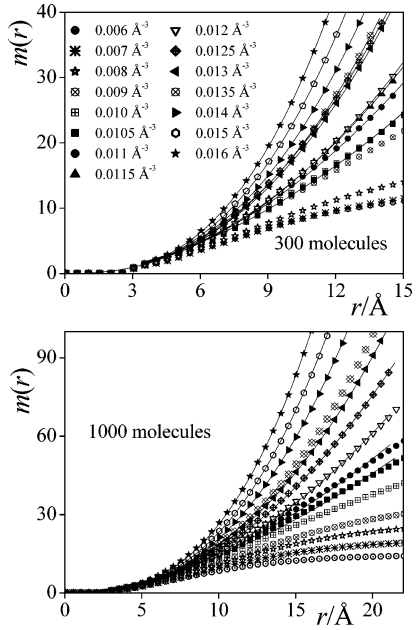

Figure 1. The $m(r)$ radial distribution (i.e., number of molecules belonging to the largest cluster of the system that are located at the distance r from another molecule of this cluster), as obtained in the systems containing 300 (top panel), and 1000 (bottom panel) water molecules at the 15 different densities considered (symbols). The curves fitted to these data (see eq 1) in the cases when the obtained $m(r)$ function does not have inflexion in the entire r range within which it is calculated are shown by full lines.

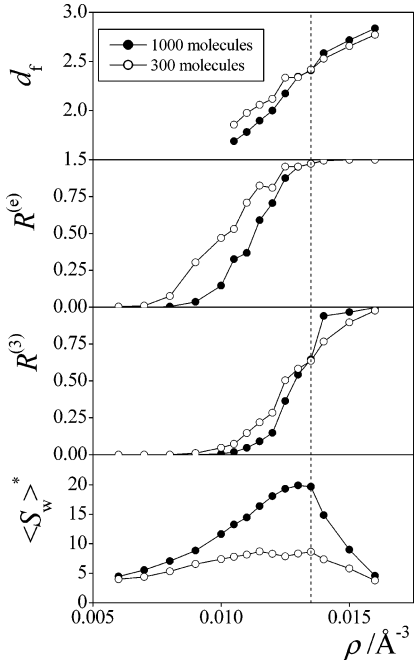

Figure 2. Variation of the fractal dimension of the largest cluster d_f (top panel), the probability of finding a cluster that spans the system in at least one dimension $R^{(e)}$ (second panel) and in all three dimensions $R^{(3)}$ (third panel), and the cluster size weight average excluding the largest cluster of the system $\langle S_w \rangle^*$ (bottom panel) with the density of the system: open circles, system containing 300 water molecules; full circles, system containing 1000 water molecules. The lines connecting the symbols are just guides to the eye. The dashed vertical line indicates the estimated percolation threshold.

the critical fractal dimension value of 2.53 in both of the systems simulated. This means that the critical density at which the true percolation transition occurs can be detected rather accurately through the fractal dimension of the largest cluster, and the

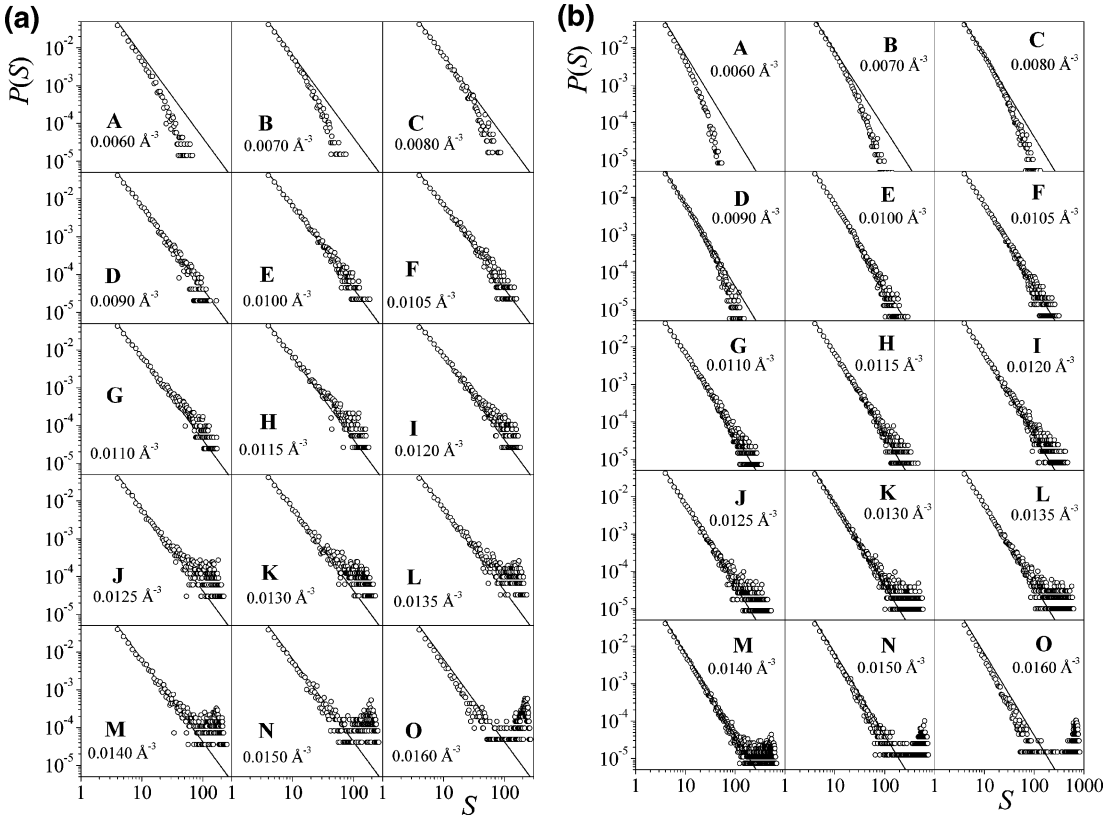

Figure 3. Size distribution of the hydrogen-bonding clusters, as obtained in the systems containing (a) 300 and (b) 1000 water molecules at the 15 different densities considered (open circles), plotted on a logarithmic scale. The solid lines show the critical curve corresponding to the power law predicted at the percolation threshold (see eq 2).

obtained percolation threshold density value is not affected by noticeable systematic error due to the finite size of the system simulated.

The threshold density obtained from the analysis of d_f agrees well with the density values at which the spanning probabilities $R^{(e)}$ and $R^{(3)}$ become equal as obtained in the two systems of different size (i.e., about 0.0130 and 0.0135 Å^{-3} for $R^{(e)}$ and $R^{(3)}$, respectively, see Figure 2 and Table 1). In accordance with our earlier findings,[54,67] namely, that the critical value of the $R^{(e)}$ spanning probability at the percolation threshold in three-dimensional aqueous systems exceeds 0.95, this critical value of $R^{(e)}$ is found to be about 0.97 here. Further, the critical value of the $R^{(3)}$ spanning probability is estimated to be 0.65 ± 0.05 (see Figure 2 and Table 1). Since the critical value of $R^{(e)}$ is rather close to 1, the location of the percolation threshold can be detected with a considerably higher accuracy through the spanning probability $R^{(3)}$ than through $R^{(e)}$, and therefore the use of $R^{(3)}$ rather than $R^{(e)}$ is recommended in such studies.

The obtained values of the cluster size weight average $\langle S_w \rangle^*$ (where the asterisk indicates that the largest cluster is excluded from the averaging) are in a full accordance with the above findings. Thus, the $\langle S_w \rangle^*(\rho)$ curve goes through a maximum at the molecular number density value of 0.0130 Å^{-3}, very close but still below the percolation threshold density (see Figure 2 and Table 1).

However, the analysis of the cluster size distributions $P(S)$, shown in Figure 3, leads to rather different estimation of the percolation threshold. As is seen, at the density value of 0.0135 Å^{-3} (i.e., in state L, which has been identified to be closest to the percolation threshold among the 15 different states considered) the obtained $P(S)$ distribution clearly exceeds the critical curve at large S values, indicating presence of a percolating cluster. The best agreement of the obtained cluster size distribution data with the critical curve of eq 2 and the appearance of a small hump at the S values comparable with the system size are found at the densities of 0.0105 Å^{-3} (state F) and 0.0115 Å^{-3} (state H) in the systems containing 300 and 1000 water molecules, respectively. The facts that (i) these densities are considerably lower than the one identified above as the true percolation threshold density and (ii) the density at which the $P(S)$ distribution obtained in the small system agrees best with eq 2 is clearly smaller than the corresponding density for the large system indicate that the threshold detected through the cluster size distribution is the point at which the linear extension of the largest cluster exceeds the size of the simulation box, and not the true percolation threshold, i.e., the point at which this cluster becomes infinitely large. This is confirmed by the finding that the density value at which the cluster size distribution $P(S)$ agrees best with eq 2 coincides in both systems with the density at which the probability of finding a spanning cluster exceeds the probability of not finding such a cluster, i.e., when the $R^{(e)}$ spanning probability exceeds 0.50, the value previously thought to indicate the percolation threshold.[53,58,70] This means that the detection of the percolation threshold through the cluster size distribution of the system, contrary to the other three methods, is affected by a systematic error due to the finite size of the system simulated, and thus the true percolation threshold is underestimated in this way.

It should also be noted that, due to the large statistical noise of the $P(S)$ distribution, the localization of the percolation threshold through $P(S)$ requires much better statistics than either through the fractal dimension of the largest cluster or the spanning probabilities. Thus, using the present data set for the smaller system, it is almost impossible to detect the density at which the $P(S)$ distribution drops below the universal power law (eq 2) at intermediate S values, which is a clear signature

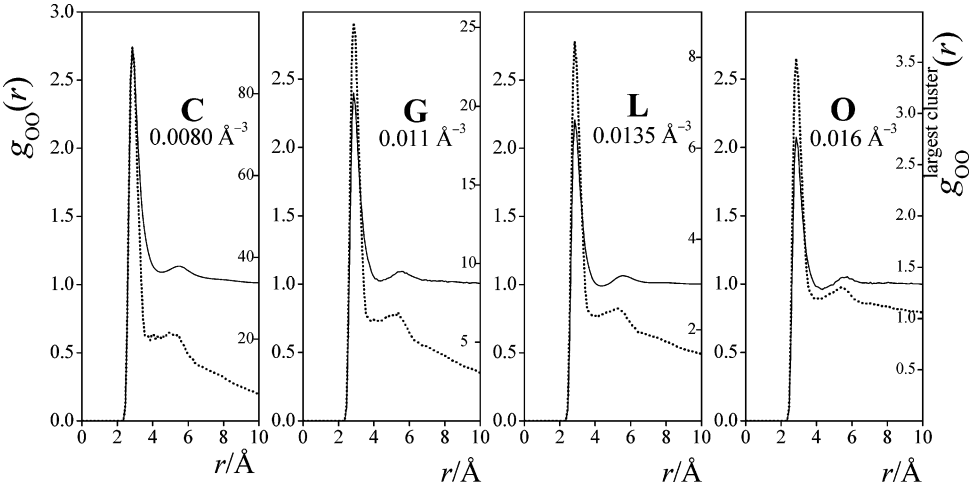

Figure 4. Oxygen−oxygen partial pair correlation function, calculated among all water molecules present in the system ($g_{OO}(r)$, solid lines) and among the water molecules belonging to the largest cluster only ($g_{OO}^*(r)$, dashed lines) in states C (left panel), G (second panel), L (third panel), and O (right panel) in the system containing 1000 water molecules. The scales on the left side of the panels correspond to the $g_{OO}(r)$, whereas those on the right side correspond to the $g_{OO}^*(r)$ functions.

that the system is above the percolation threshold. Such a drop can only be seen in the $P(S)$ distribution of considerably larger systems and, indeed, may be noticed in states N and O of the system containing 1000 water molecules (see Figure 3b).

Finally, it should be noted that the density at which the true percolation transition is found to occur, i.e., 0.0137 ± 0.0003 Å^{-3} (0.410 ± 0.009 g/cm^3), is higher than the density of 0.0129 Å^{-3} (0.386 g/cm^3), obtained at the pressure of 40 MPa along the 700 K isotherm in the system that has been misidentified as percolating in a previous paper through the agreement of the $P(S)$ distribution with the critical line and the $R^{(e)}$ spanning probability value of 0.5.[53] In the light of the present results the system in this state, located already above the supercritical extension of the boiling line of the SPC/E water model,[53] should be still regarded as nonpercolating. Thus, the present results show that, contrary to our earlier claims,[53] the line of percolation of the hydrogen-bonded clusters in supercritical water goes through pressures/densities that are somewhat higher than the values corresponding to the supercritical extension of the vapor−liquid coexistence curve (the latter being estimated on the basis of the pioneering results of Guissani and Guillot[71]).

3.2. Characterization of the Largest Cluster Around the Percolation Threshold. In order to characterize the structure of the largest cluster at the vicinity of the percolation threshold, we have calculated the oxygen−oxygen pair correlation function of the molecules belonging to the largest cluster $g_{OO}^*(r)$ in the system containing 1000 water molecules. (The asterisk in $g_{OO}^*(r)$ indicates that only the pairs of molecules both of which belong to the largest cluster of the system contribute to this function.) The $g_{OO}^*(r)$ functions obtained in states C, G, L, and O are shown in Figure 4, together with the full $g_{OO}(r)$ pair correlation functions, calculated considering all water molecules of the system. Besides their main peak at about 2.9 Å, corresponding to the hydrogen-bonded water pairs, all the shown pair correlation functions exhibit a second peak nearly at the double of this distance, i.e., around 5.5 Å. The presence of this peak indicates the dominance of nearly linear chainlike arrangements of the water molecules, in a clear contrast with the $g_{OO}(r)$ function of water at ambient conditions,[22,23,26] where the second peak appears at about 4.5 Å due to the tetrahedral arrangement of the molecules.

The topology of the largest cluster is found to be rather insensitive to the density of the system around the percolation

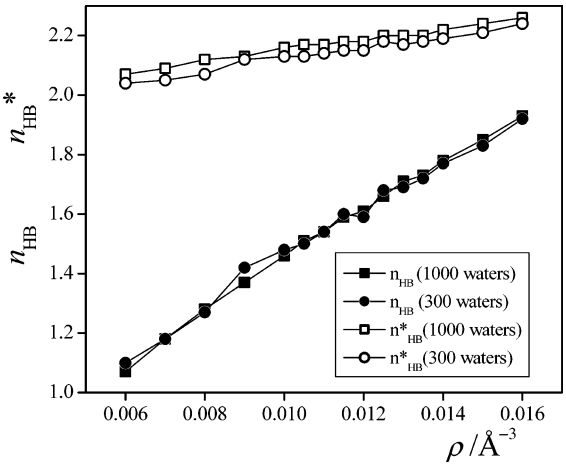

Figure 5. Density dependence of the average number of hydrogen bonds a water molecule forms with its neighbors, as calculated among all water molecules (n_{HB}, filled symbols) and among the water molecules belonging to the largest cluster only (n_{HB}*, open symbols) in the systems containing 300 (circles) and 1000 (squares) water molecules.

threshold, as indicated by a very slow change of the average number of hydrogen bonds a water molecule belonging to the largest cluster forms (n_{HB}*, where the asterisk again refers to the fact that this quantity is calculated only within the largest cluster). The change of n_{HB}* and n_{HB} (i.e., the average number of hydrogen bonds a water molecule of the system forms, irrespective of whether it belongs to the largest cluster or not) with the density is shown in Figure 5, while the obtained n_{HB}* and n_{HB} values are also summarized in Table 1. As is seen, the number of hydrogen bonds increases much slower within the largest cluster than within the entire system when the density is increased. Thus, the increase of the density of the system from 0.006 to 0.016 Å^{-3} (i.e., moving from state A to O) is accompanied by a 75−80% increase of the number of hydrogen bonds per molecule within the entire system but only by a 9−10% increase of it within the largest cluster. This finding indicates that the topology of the large water clusters is rather similar in the entire density range investigated, corresponding to cluster sizes ranging from a few tens or hundreds of water molecules up to infinity. Instead, the effect of the increasing density is to attach more and more clusters together via formation of new hydrogen bonds, progressively increasing the

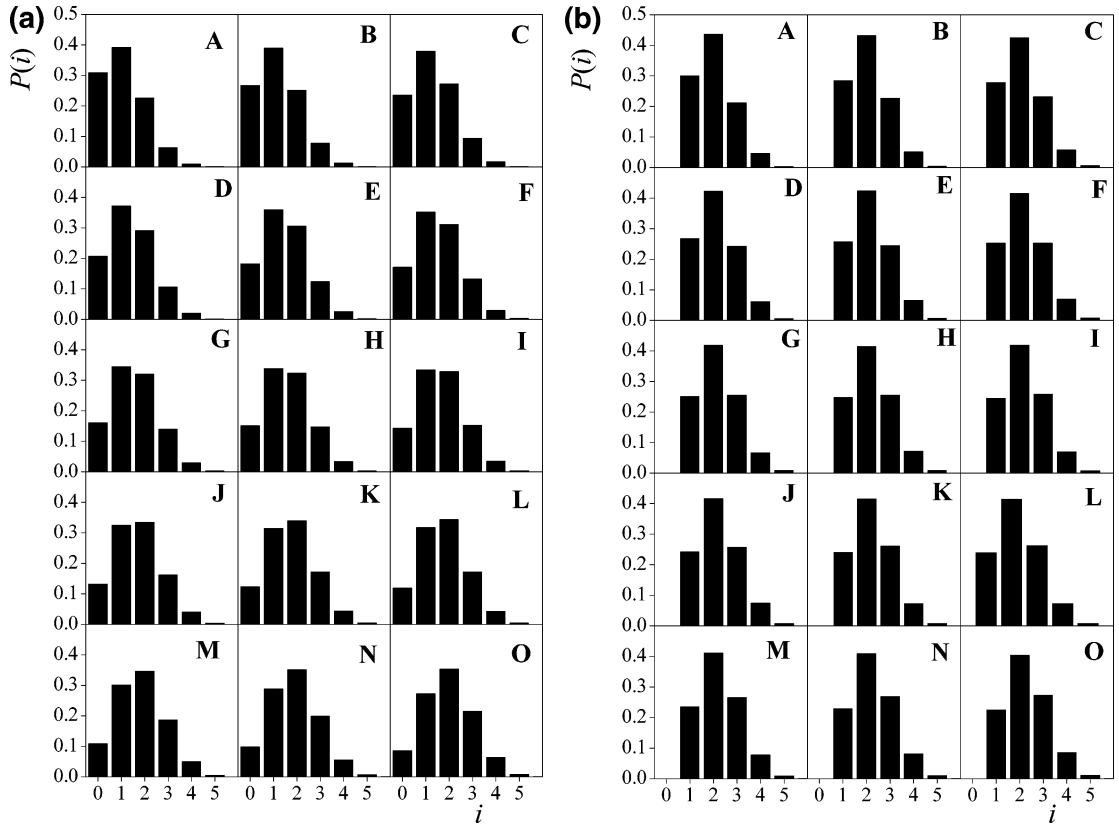

Figure 6. Distribution of the water molecules according to their hydrogen-bonded neighbors *i*, as calculated (a) among all water molecules and (b) among the water molecules belonging to the largest cluster only in the system containing 1000 water molecules.

size of the largest cluster of the system until it becomes infinite at the percolation threshold.

Similar conclusions can be drawn from the $P(i)$ distribution of the water molecules according to the number of their hydrogen-bonded neighbors i. The $P(i)$ distributions calculated within the largest cluster and among all the molecules of the large system at different densities are shown in Figure 6. As is seen, the distribution changes much slower when only the molecules within the largest cluster are considered than in the case of taking all molecules of the system into account. It is also seen that within the largest cluster of the system the largest fraction, i.e., about 40−44% of the water molecules, has exactly two hydrogen-bonded neighbors in the entire density range investigated, the fractions of the molecules having one and three hydrogen-bonded neighbors are equally about 23−27%, whereas 6−10% of the molecules have more than three hydrogen-bonded neighbors.

4. Summary and Conclusions

In this article we have presented a detailed analysis of the percolation transition of water along a supercritical isotherm. Besides the localization of the percolation threshold and characterization of the large, mesoscopic water clusters present in supercritical water at the vicinity of the percolation threshold, methodological issues concerning the localization of the true percolation threshold have also been addressed. Thus, it has been demonstrated that the determination of the fractal dimension of the largest cluster present in the system as well as the calculation of various spanning probabilities can be used to determine the percolation threshold at which a truly infinite cluster appears in the system. This point can be characterized by the critical fractal dimension value of 2.53 and by the fact that the spanning probabilities determined in systems of different size become equal to each other. Considering the spanning rules that the largest cluster spans the system (i) in at least one dimension and (ii) in all three dimensions the critical spanning probabilities at which this occurs are found to be about 0.97 and 0.65, respectively. Contrary to these two methods, the cluster size distribution can hardly be used to detect the percolation threshold, since it is distorted in a wide range of cluster sizes due to the finite size of the system simulated. Thus, the threshold value provided by this method corresponds to the point at which the linear extension of the largest cluster exceeds the size of the system rather then where it becomes infinitely large, and hence the location of the percolation threshold is systematically underestimated this way.

The point at which the true percolation transition occurs is found to be at a somewhat higher density than the value corresponding to the extension of the vapor−liquid coexistence line of the used water model above the critical point. This deviation may be even larger due to the difference of the hydrogen-bonded and physical clusters, which is negligible at ambient conditions, but becomes noticeable at temperatures above the critical point. It should be noted that this difference cannot be solely attributed to the inaccuracy of the calculated critical density value of SPC/E water, which can be estimated to be about 0.01 g/cm^3 (since the values that are reported in the literature are scattering between 0.273 and 0.295 g/cm^3),[71−73] whereas the density value at which the percolation transition occurs along the 700 K isotherm, i.e., 0.410 g/cm^3, is at least 0.024 g/cm^3 higher than the density corresponding to the supercritical extension of the boiling line at this temperature.[53]

In analyzing the properties of the largest cluster of the system we have found that the structure of this cluster is dominated by linear, chainlike arrangements of water molecules and also that its topology does not change considerably with the density of

the system in the entire density range investigated. Instead, the increase of the density results in the rapid growth of the largest cluster as more and more clusters of similar topology are attached to it via formation of new hydrogen bonds up to the percolation threshold, where this cluster becomes infinitely large.

Acknowledgment. This work has been supported by the Hungarian OTKA Foundation under Project No. T049673. P.J. is a Békésy György fellow of the Hungarian Ministry of Education, which is gratefully acknowledged. A.O. and I.B. thank DFG (FG 436) for financial support.

References and Notes

(1) Franck, E.; Roth, K. *Discuss. Faraday Soc.* **1967**, *42*, 108.
(2) Gorbaty, Y. E.; Demianets, Y. N. *Chem. Phys. Lett.* **1983**, *100*, 450.
(3) Bondarenko, G. V.; Gorbaty, Y. E. *Mol. Phys.* **1991**, *74*, 639.
(4) Kalinichev, A. G. *Z. Naturforsch.* **1991**, *46a*, 433.
(5) Cummings, P. T.; Cochran, H. D.; Simonson, J. M.; Mesmer, R. E.; Karaborni, S. *J. Chem. Phys.* **1991**, *94*, 5607.
(6) Postorino, P.; Tromp, R. H.; Ricci, M. A.; Soper, A. K.; Neilson, G. W. *Nature* **1993**, *366*, 668.
(7) Postorino, P.; Ricci, M. A.; Soper, A. K. *J. Chem. Phys.* **1994**, *101*, 4123.
(8) Chialvo, A. A.; Cummings, P. T. *J. Chem. Phys.* **1994**, *101*, 4466.
(9) Tromp, R. H.; Postorino, P.; Neilson, G. W.; Ricci, M. A.; Soper, A. K. *J. Chem. Phys.* **1994**, *101*, 6210.
(10) Fois, E. S.; Sprik, M.; Parrinello, M. *Chem. Phys. Lett.* **1994**, *223*, 411.
(11) Löffler, G.; Schreiber, H.; Steinhauser, O. *Ber. Bunsen-Ges. Phys. Chem.* **1994**, *98*, 1575.
(12) Kalinichev, A. G.; Bass, J. D. *Chem. Phys. Lett.* **1994**, *231*, 301.
(13) Mizan, T. I.; Savage, P. E.; Ziff, R. M. *J. Phys. Chem.* **1994**, *98*, 13067.
(14) Yamanaka, K.; Yamaguchi, T.; Wakita, H. *J. Chem. Phys.* **1994**, *101*, 9830.
(15) Gorbaty, Y. E.; Kalinichev, A. K. *J. Phys. Chem.* **1995**, *99*, 5336.
(16) Jedlovszky, P.; Vallauri, R. *J. Chem. Phys.* **1996**, *105*, 2391.
(17) Svishchev, I. M.; Kusalik, P. G.; Wang, J.; Boyd, R. J. *J. Chem. Phys.* **1996**, *105*, 4742.
(18) Mizan, T. I.; Savage, P. E.; Ziff, R. M. *J. Phys. Chem.* **1996**, *100*, 403.
(19) Chialvo, A. A.; Cummings, P. T. *J. Phys. Chem.* **1996**, *100*, 1309.
(20) Chialvo, A. A.; Cummings, P. T. *J. Phys.: Condens. Matter* **1996**, *8*, 9281.
(21) Kalinichev, A. G.; Bass, J. D. *J. Phys. Chem. A* **1997**, *101*, 9720.
(22) Soper, A. K.; Bruni, F.; Ricci, M. A. *J. Chem. Phys.* **1997**, *106*, 247.
(23) Bellissent-Funel, M. C.; Tassaing, T.; Zhao, H.; Beysens, D.; Guillot, B; Guissani, Y. *J. Chem. Phys.* **1997**, *107*, 2942.
(24) Hoffmann, M. M.; Conradi, M. S. *J. Am. Chem. Soc.* **1997**, *119*, 3811.
(25) Ricci, M. A.; Nardone, M.; Fontana, A.; Andreani, C.; Hahn, W. *J. Chem. Phys.* **1998**, *108*, 450.
(26) Jedlovszky, P.; Brodholt, J. P.; Bruni, F.; Ricci, M. A.; Soper, A. K.; Vallauri, R. *J. Chem. Phys.* **1998**, *108*, 8528.
(27) Botti, A.; Bruni, F.; Ricci, M. A.; Soper, A. K. *J. Chem. Phys.* **1998**, *109*, 3180.
(28) Tassaing, T.; Bellissent-Funel, M. C.; Guillot, B.; Guissani, Y. *Europhys. Lett.* **1998**, *42*, 265.
(29) Yoshii, N.; Yoshie, H.; Miura, S.; Okazaki, S. *J. Chem. Phys.* **1998**, *109*, 4873.
(30) Dang, L. X. *J. Phys. Chem. B* **1998**, *102*, 620.
(31) Yoshie, H.; Miura, S.; Okazaki, S. *Bull. Chem. Soc. Jpn.* **1999**, *72*, 151.
(32) Mountain, R. D. *J. Chem. Phys.* **1999**, *110*, 2109.
(33) Okada, K.; Yao, M.; Hiejima, Y.; Kohno, H.; Kajihara, Y. *J. Chem. Phys.* **1999**, *110*, 3026.
(34) Martí, J. *J. Chem. Phys.* **1999**, *110*, 6876.
(35) Matubayasi, N.; Wakai, C.; Nakahara, M. *J. Chem. Phys.* **1999**, *110*, 8000.
(36) Kalinichev, A. G.; Churakov, S. V. *Chem. Phys. Lett.* **1999**, *302*, 411.
(37) Jedlovszky, P.; Richardi, J. *J. Chem. Phys.* **1999**, *110*, 8019.
(38) Jedlovszky, P. *J. Chem. Phys.* **1999**, *111*, 5975.
(39) Walrafen, G. E.; Yang, W. H.; Chu, Y. C. *J. Phys. Chem. B* **1999**, *103*, 1332.
(40) Bonetti, M.; Romet-Lemonne, G.; Calmettes, P.; Bellissent-Funel, M. C. *J. Chem. Phys.* **2000**, *112*, 268.
(41) Morita, T.; Kusano, K.; Ochiai, H.; Saitow, K.; Nishikawa, K. *J. Chem. Phys.* **2000**, *112*, 4203.
(42) Tassaing, T.; Bellissent-Funel, M. C. *J. Chem. Phys.* **2000**, *113*, 3332.
(43) Skaf, M. S.; Laria, D. *J. Chem. Phys.* **2000**, *113*, 3499.
(44) Khan, A. *J. Phys. Chem. B* **2000**, *104*, 11268.
(45) Marcus, Y. *Phys. Chem. Chem. Phys.* **2000**, *2*, 1465.
(46) Richardi, J.; Jedlovszky, P.; Fries, P. H.; Millot, C. *J. Mol. Liq.* **2000**, *87*, 177.
(47) Jedlovszky, P.; Vallauri, R.; Richardi, J. *J. Phys.: Condens. Matter* **2000**, *12*, A115.
(48) Uffindell, C. H.; Kolesnikov, A. I.; Li, J. C.; Mayers, J. *Phys. Rev. B* **2000**, *62*, 5492.
(49) Lotfollahi, M. N.; Modarres, H.; Mansoori, G. A. *J. Phys. Chem. B* **2001**, *105*, 9834.
(50) Matubayasi, N.; Nakao, N.; Nakahara, M. *J. Chem. Phys.* **2001**, *114*, 4107.
(51) Boero, M.; Terakura, K.; Ikeshoji, T.; Liew, C. C.; Parrinello, M. *J. Chem. Phys.* **2001**, *115*, 2219.
(52) Akiya, N.; Savage, P. E. *Chem. Rev.* **2002**, *102*, 2725.
(53) Pártay, L.; Jedlovszky, P. *J. Chem. Phys.* **2005**, *123*, 024502.
(54) Pártay, L.; Jedlovszky, P.; Brovchenko, I.; Oleinikova, A. *Phys. Chem. Chem. Phys.* **2007**, *9*, 1341.
(55) Geiger, A.; Stillinger, F.; Rahman, A. *J. Chem. Phys.* **1979**, *70*, 4185.
(56) Stanley, H. E.; Teixeira, J. *J. Chem. Phys.* **1980**, *73*, 3404.
(57) Bruni, F.; Ricci, M. A.; Soper, A. K. *Phys. Rev. B* **1996**, *54*, 11876.
(58) Padró, J. A.; Martí, J.; Guàrdia, E. *J. Phys.: Condens. Matter* **1994**, *6*, 2283.
(59) Coniglio, A.; Klein, W. *J. Phys. A: Math. Gen.* **1980**, *13*, 2775.
(60) Hill, T. L. *J. Chem. Phys.* **1955**, *23*, 617.
(61) Berendsen, H. J. C.; Grigera, J. R.; Straatsma, T. P. *J. Phys. Chem.* **1987**, *91*, 6269.
(62) Jedlovszy, P.; Vallauri, R. *J. Chem. Phys.* **2005**, *122*, 081101.
(63) Barker, J. A.; Watts, R. O. *Mol. Phys.* **1973**, *26*, 789.
(64) Neumann, M. *J. Chem. Phys.* **1985**, *82*, 5663.
(65) Jan, N. *Physica A* **1999**, *266*, 72.
(66) Hovi, J. P.; Aharony, A. *Phys. Rev. E* **1996**, *53*, 235.
(67) Oleinikova, A.; Brovchenko, I. *J. Phys.: Condens. Matter* **2006**, *18*, S2247.
(68) Stauffer, D. *Introduction to Percolation Theory*; Taylor and Francis: London, 1985.
(69) Oleinikova, A.; Brovchenko, I.; Geiger, A.; Guillot, B. *J. Chem. Phys.* **2002**, *117*, 3296.
(70) Martins, P. H. L.; Plascak, J. A. *Phys. Rev. E* **2003**, *67*, 046119.
(71) Guissani, Y.; Guillot, B. *J. Chem. Phys.* **1993**, *98*, 8221.
(72) Boulougouris, G. C.; Economou, I. G.; Theodorou, D. N. *J. Phys. Chem. B* **1998**, *102*, 1029.
(73) Errington, J. D.; Panagiotopoulos, A. Z. *J. Phys. Chem. B* **1998**, *102*, 7470.